Supporting Information

Tailor-Made Pyrazolide-Based Metal-Organic Frameworks for Selective Catalysis

Ning Huang,[†] Kecheng Wang,[†] Hannah Drake,[†] Peiyu Cai,[†] Jiandong Pang,[†] Jialuo Li,[†] Sai Che,[†] Lan Huang,[§] Qi Wang,[†] and Hong-Cai Zhou[†,*]

[†]Department of Chemistry, Texas A&M University, College Station, Texas 77842-3012, United States

[§]Department of Materials Science and Engineering, Texas A&M University, College Station, Texas 77843-3003, United States

E-mail: zhou@chem.tamu.edu

Table of Contents

Section 1. Methods

^{1}H-NMR spectra were measured on Mercury NMR spectrometer, where chemical shifts (δ in ppm) were determined with a residual proton of the solvent as standard. Powder X-ray diffraction (PXRD) experiments were carried out on a BRUKER D8-Focus Bragg-Brentano X-ray powder. Diffractometer equipped with a Cu sealed tube (λ = 1.54178 Å) at 40 kV and 40 mA. Fourier transform infrared (FT-IR) spectra were recorded on an IR Affinity-1 instrument. Thermogravimetric analysis (TGA) data were obtained on a TGA-50 (SHIMADZU) thermogravimetric analyzer with a heating rate of 10 °C min^{-1} under air atmosphere. N_2 adsorption−desorption isotherms were measured using a Micromeritics ASAP 2420 system at 77 K. The UV−vis absorption spectra were recorded on a Shimadzu UV-2450 spectrophotometer. The morphologies of the MOF sample were observed by using a SU8020 Scanning Electron Microscope (SEM, Hitachi, Japan). Elemental analysis (EA) was performed by vario EL cube Elementar. Inductively Coupled Plasma-Optical Emission spectroscopic (ICP-OES) data were collected on a Thermo iCAP-6300 Spectrometer. The conversions of the reactants and the yields of products were measured by Shimadzu QP2100 plus high pressure liquid chromatography-mass spectrometry (HPLC-MS).

C_{70} was employed as an internal standard for the quantitative HPLC analysis. The standard toluene solutions of anthracene, C_{60}, C_{70}, $C_{60}An$, $C_{60}An_2$, and $C_{60}An_3$ were prepared. The mixture of a fixed amount of internal standard and calibration standards were prepared and analyzed. The peak areas of C_{70} and each analyte sample were recorded and calculated. The linear calibration was calculated according to the following formula:

$$\frac{A_a}{A_i} = \frac{mC_a}{C_i} + \mathrm{b}$$

Then the mixture of the internal standard (C_{70}) and the analyte sample was prepared. The concentration of the analyte sample can be measured by rearranging the formula to:

$$C_a = \frac{C_i}{m}[(A_a/A_i) - b]$$

A = peak area

C = concentration

i = internal standard

a = analyte

m = slope

b = intercept

The simulation were determined using the density-functional tight-binding (DFTB+) method including Lennard-Jones (LJ) dispersion. The calculations were carried out with the DFTB+ program package version 1.29. DFTB is an approximate density functional theory method based on the tight binding approach and utilizes an optimized minimal LCAO Slater-type all-valence basis set in combination with a two-center approximation for Hamiltonian matrix elements. The Coulombic interaction between partial atomic charges was determined using the self-consistent charge (SCC) formalism. Lennard-Jones type dispersion was employed in all calculations to describe van der Waals (vdW) and π-stacking interactions. The lattice dimensions were optimized simultaneously with the geometry. Standard DFTB parameters for X–Y element pair (X, Y = C, H, F, and N) interactions were employed from the mio-0-1 set10. The accessible volume for guest molecules was calculated from the Monte Carlo integration technique using a probe molecule (diameter = 2.8 Å) roll over the framework surface with a grid interval of 0.25 Å.

Section 2. Materials and Synthetic Procedures

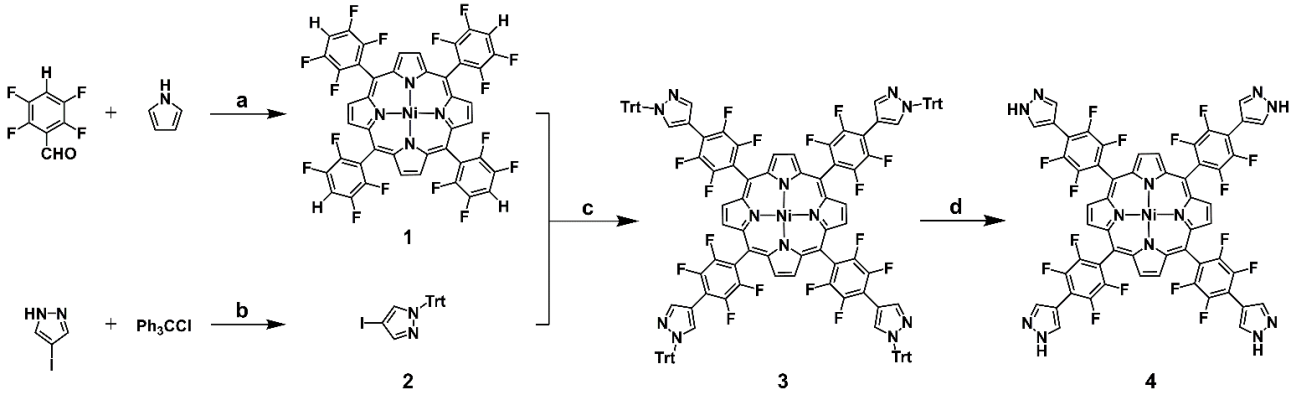

[a]Reaction conditions: (a) i. CH_2Cl_2, CF_3COOH, r.t., 48 h; ii. DDQ, r.t., overnight, 22%; iii. $Ni(OAc)_2$, DMF, reflux, overnight, 87%. (b) Trityl chloride, Et_3N, CH_2Cl_2, reflux, 48 h, 82%. (c) i. $Pd(PPh_3)_4$, *t*-BuOLi, CuCl, DMF, 100 °C, 72 h, 75%. (d) i. CF_3COOH, $CHCl_3$, 24 h, 56%; ii. Boc_2O, Et_3N, CH_2Cl_2, 72 h, 80%; iii. DMF, MeOH, 80 °C, 48 h, 85%.

Synthesis of free base tetrakis(2,3,5,6-tetrafluorophenyl)-porphyrin. Into a 500 mL round bottom flask, tetrafluorobenzaldehyde (5.56 g, 31.2 mmol) and pyrrole (2.08 g, 31.2 mmol) were dissolved in dichloromethane (160 mL) and purged with N_2 for 15 min. BF_3•OEt_2 (890 µL, 7.05 mmol) was then added to the reaction mixture. The reaction mixture was stirred at room temperature for 48 h. And then DDQ (11.6 g, 51.0 mmol) was added and stirred overnight. The crude reaction mixture was filtered with silica gel and then concentrated under vacuum. Purification by silica gel chromatography using pure dichloromethane gave the product. The product was then washed with MeOH (5 mL). The mixture was filtered and a purple solid product was collected which was then suction-dried for 1 h to afford 1.83 g product (yield = 24%). ^{1}HNMR (400 MHz, $CDCl_3$) δ = 8.92 (s, 8H), 7.68−7.60 (m, 4H), −2.87 (s, 2H). ^{19}FNMR (375 MHz, $CDCl_3$) δ = −137.24 (m, 8F), −138.57 (m, 8F). MALDI-TOF MS: m/z 902.10 (903.21 calcd for $[M+H]^+$).

Synthesis of tetrakis(2,3,5,6-tetrafluorophenyl)-porphyrin nickel (II) (1). Tetrakis(2,3,5,6-tetrafluorophenyl)-porphyrin (4.0 g, 4.43 mmol), $Ni(OAc)_2$ (2.65 g, 13.3 mmol), and *N*,*N*-dimethylformaldehyde (300 mL) were added into a 500 mL flask. The flask was attached with a water condenser. The reaction mixture was heated to reflux for 12 h. The reaction mixture was cooled down to room temperature and poured in to 500 mL water. The precipitated product

from the mixture was isolated by filtration. The crude product was then purified by neutral alumina column chromatography to obtain a purple product (4.88 g, yield = 87%). MALDI-TOF MS: m/z = 958.02 (958.546 calcd for $[M\cdot]^+$).

Synthesis of 4-iodo-1-trityl-pyrazole (2). 4-iodo-1*H*-pyrazole (5.0 g, 25.8 mmol) was dissolved in 80 mL of CH_2Cl_2 and the mixture was added to a dried 200 mL three-neck round bottom flask. Et_3N (4.5 mL) was then added dropwise to the reaction mixture at 0 °C and a water condenser was attached to the flask. The mixture was heated to reflux, and cautiously stirred for 30 min to give a clear colorless solution. Tritylchloride (7.2 g, 25.8 mmol) was added to the solution and the reaction was proceeded for another 24 h. The reaction system was cooled to room temperature, and then poured over 100 mL of ice water in a 1 L beaker. The resulting solution was extracted three times with CH_2Cl_2 (300 mL total). The organic phase was collected and dried over anhydrous $MgSO_4$ for 10 min. The solvents were removed by rotary evaporation and crystallized from dichloromethane/hexane solution to give 4-iodo-1-trityl-pyrazole (**2**, 8.2 g, 68% yield based on 4-iodo-1*H*-pyrazole). ^{1}H NMR (300 MHz, DMSO-d_6): δ (ppm) = 6.79-7.07 (m, 6H), 7.32-7.41 (m, 9H), 7.44 (d, 1H), 7.74 (d, 1H). ^{13}C NMR (75 MHz, DMSO-d_6): δ (ppm) = 57.42, 78.53, 127.84, 129.49, 135.99, 142.36, 144.23.

Synthesis of (3). CuCl (2.08 g, 21 mmol) and *t*-BuOLi (1.34 g, 21 mmol) were added into a 500 ml screw cap pressure vessel equipped with magnetic stir bar. And then dry DMF (120 ml) was added. The reaction vessel was sealed and taken out of the glovebox, sonicated for 5 min and then vigorously stirred at 25 °C for 1 h. The pressure vessel was placed back inside the glovebox. **1** (5.0 g, 5.22 mmol) was added in one portion, the reaction vessel was sealed, taken out of the glovebox, sonicated for 5 min and vigorously stirred at 25 °C for 1 h. The pressure vessel was placed back inside the glovebox. $Pd(PPh_3)_4$ (230 mg, 0.2 mmol) was added, followed by *N*-trityl-4-iodopyrazole (**3**, 9.33 g, 21.4 mmol).[S1] The reaction mixture was sealed, taken out of the glovebox and then placed inside an oil bath preheated to 100 °C, where it was stirred vigorously for 48 h. After cooling down to room temperature, diluted with $CHCl_3$ (200 ml) and 3% aqueous citric acid (100 ml) was added. Reaction mixture was filtered through the plug of Celite to remove CuBr. Filter cake was washed with additional CH_2Cl_2 (3 × 20 ml). Combined organic layers were separated and washed

with deionized water (5 × 100 ml), followed by brine (100 ml). Finally, the organic layer was dried over anhydrous $MgSO_4$, filtered and dry absorbed on silica gel. After purification by column chromatography on silica gel using $CHCl_3$/EtOAc (gradient from 50 to 90% of CH_2Cl_2) as eluent and evaporation of the fractions containing the product, title compound was obtained as a purple powder (9.25 g, 81%). R_f = 0.27 (SiO_2, EtOAc/CH_2Cl_2 1/1). MALDI-TOF MS: m/z = 2190.54. (2191.34 calculated for $[M+H]^+$).

Synthesis of TTFPPP (4). A 250 ml flask equipped with a magnetic stir bar was charged with compound **3** (6.0 g, 2.74 mmol) and $CHCl_3$ (50 ml). The resulting clear solution was stirred vigorously and trifluoroacetic acid (4 ml) was added, resulting in a color change from red to dark brown. Stirring was continued at 25 °C for 36 h. The resulting salt that was formed during the reaction was filtered off and washed with fresh $CHCl_3$ (3 × 10 ml). Obtained purple solid was dried in vacuum for 2 h. A 250 ml flask equipped with a magnetic stir bar was charged with this isolated salt and CH_2Cl_2 (100 ml) was added. The resulting suspension was treated with Et_3N (3 ml), followed by the addition of 4-(dimethylamino)pyridine (0.41 g, 3.33 mmol). To the open flask Boc_2O (4.0 g, 17 mmol) was added via a syringe over 5 min. (*CAUTION*: rapid evolution of CO_2 is observed during the addition! After addition of Boc_2O was complete, the reaction flask was capped with a septum connected to a bubbler. Reaction mixture was stirred vigorously at 25 °C until the evolution of CO_2 ceased). Upon completion, the reaction mixture was dry absorbed on silica gel. After purification by column chromatography on silica gel (using EtOAc/$CHCl_3$ as eluent) and evaporation of the fractions containing the product, a purple solid was obtained. Finally, the purple solid was added into a mixture of DMF (30 mL) and methanol (50 mL) and heated at 80 °C for 24 h. After cooling down to room temperature, the mixture was poured into water and extracted with chloroform (3 × 50 ml). The combined organic layer was dried over anhydrous $MgSO_4$, filtered and dry-absorbed on silica gel. After purification by column chromatography on silica gel using EtOAc/$CHCl_3$ (gradient from 50 to 90% of EtOAc) as an eluent and evaporation of the fractions containing the product, title compound was obtained as a purple powder (2.81 g, 84%). R_f = 0.23 (SiO_2, EtOAc/$CHCl_3$ 2/1). MALDI-TOF MS: m/z = 1222.10. (1222.62 calculated for $[M\cdot]^+$).

Synthesis of C_{60}-anthracene adducts. Fullerene C_{60} (100 mg, 138.8 μmol) and anthracene (49.5

mg, 277.6 μmol) were added into toluene (30 mL) under argon atmosphere and heated at 50 °C overnight. The reaction mixture was cooled down to room temperature and the solvent was evaporated under vacuum. The mixture of mono-($C_{60}An$), bis-($C_{60}An_2$) and tris-adducts ($C_{60}An_3$) was obtained after purification by repeated preparative thin-layer chromatography (CS_2/hexane = 3/1) in the yields of 23% (27.6 mg), 19% (28.4 mg), and 3% (5.22 mg), respectively. The characterization was in agreement with previously reported data.[S2,S3]

Section 3. Supporting Figures

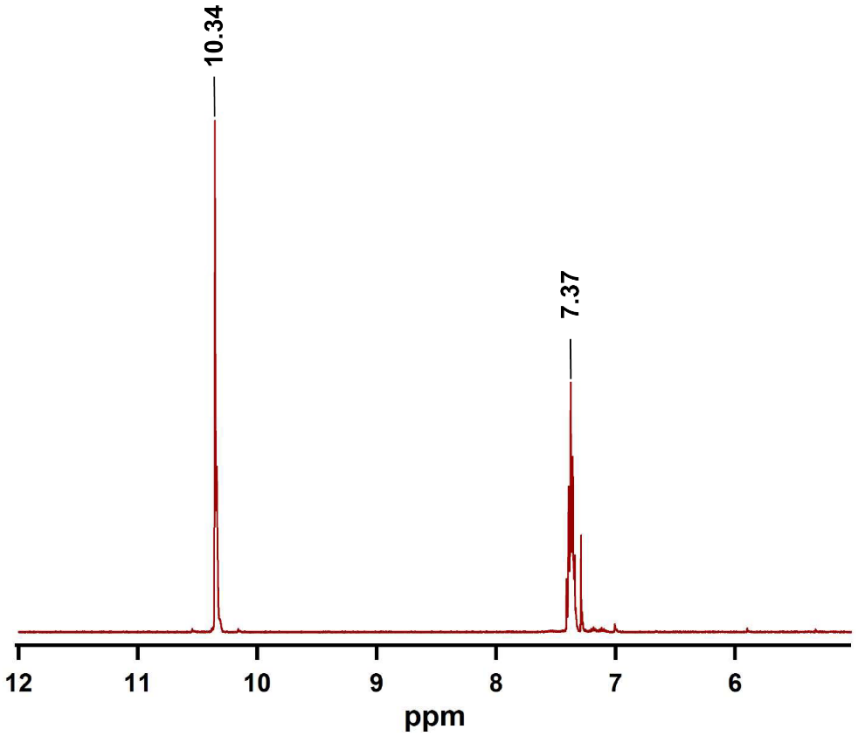

Figure S1. ^{1}H NMR spectrum of tetrafluorobenzaldehyde.

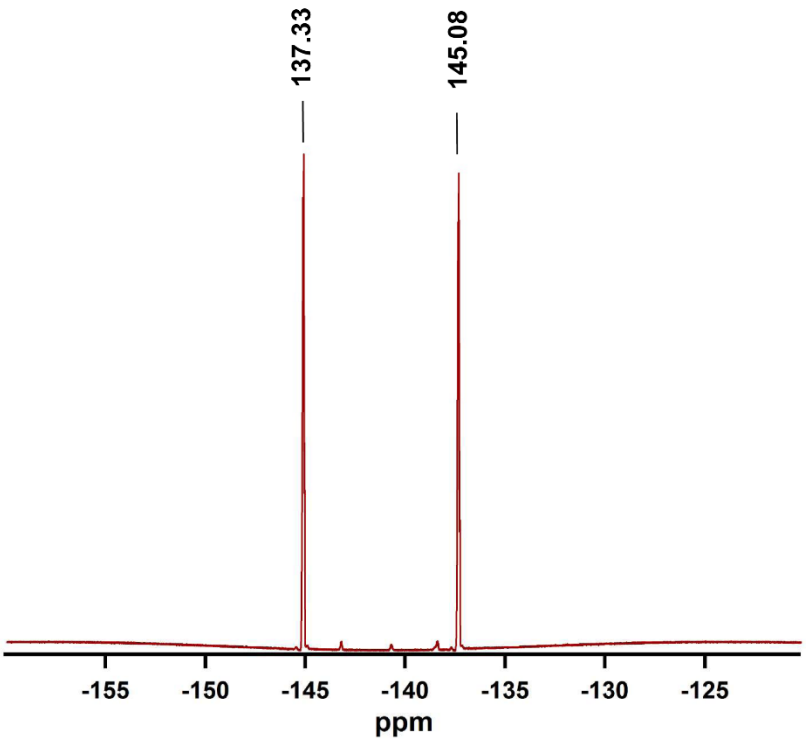

Figure S2. ^{19}F NMR spectrum of tetrafluorobenzaldehyde.

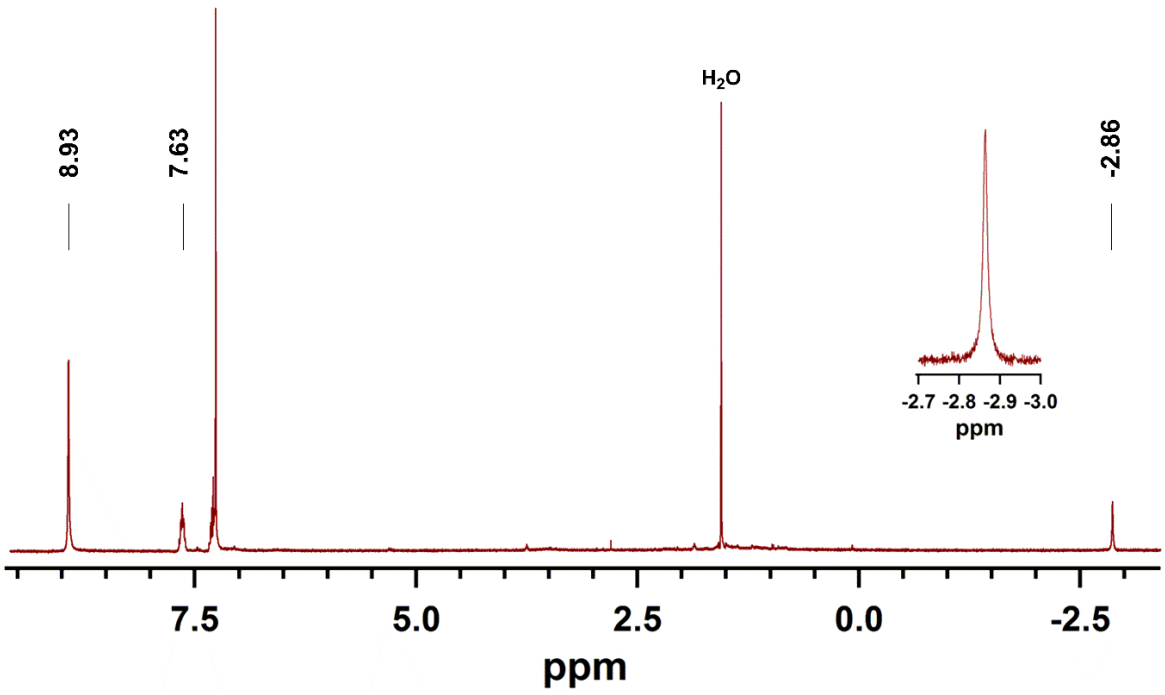

Figure S3. [1]H NMR spectrum of the free base porphyrin **1**.

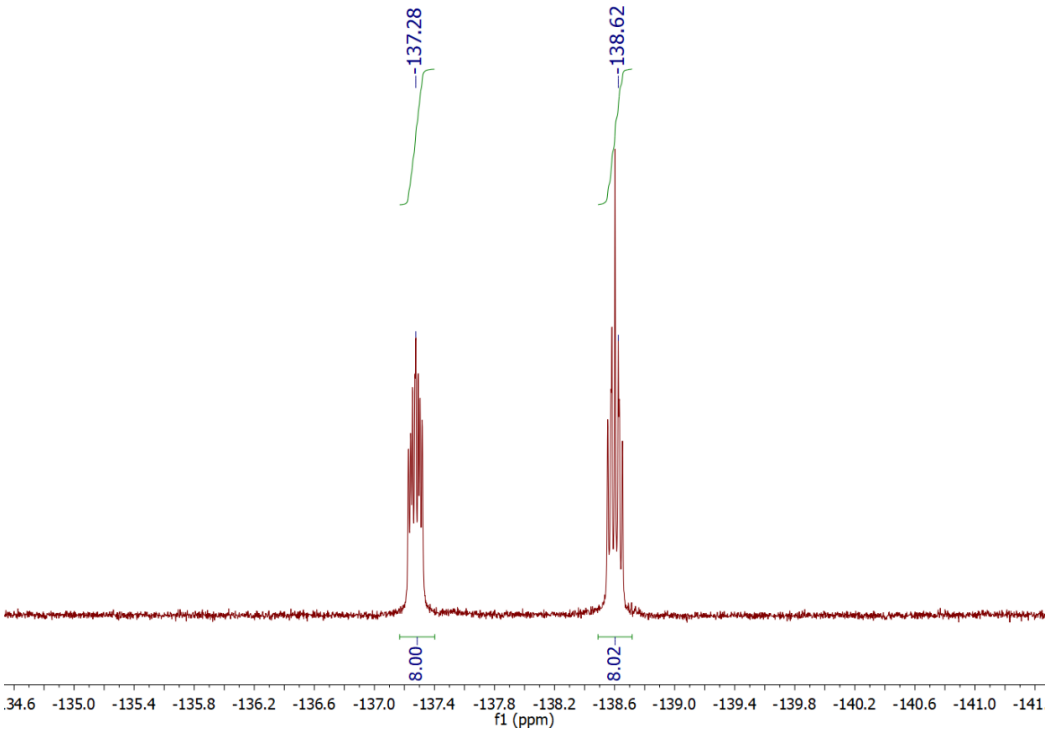

Figure S4. [19]F NMR spectrum of the free base porphyrin **1**.

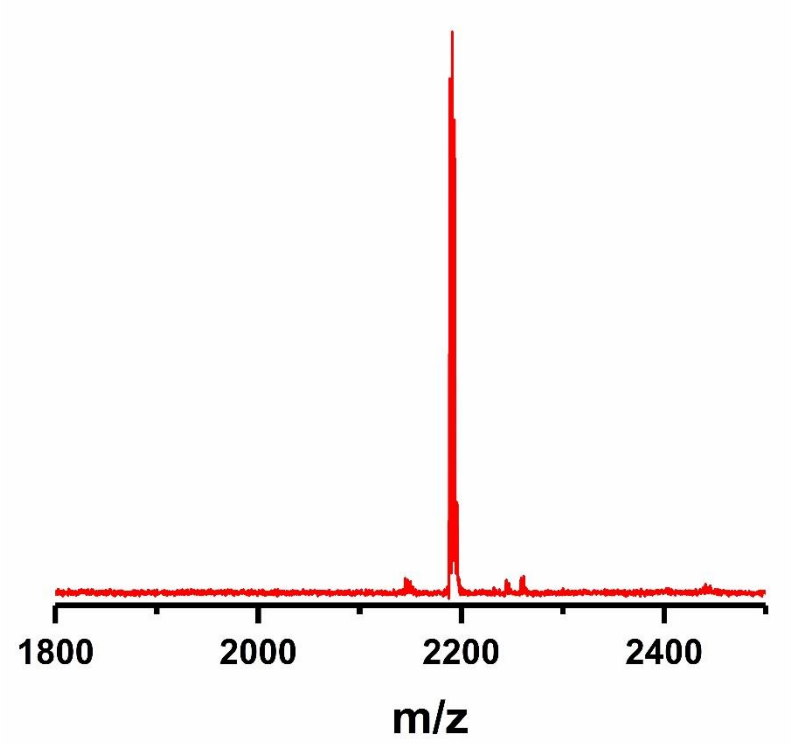

Figure S5. MALDI-TOF spectrum of **3**.

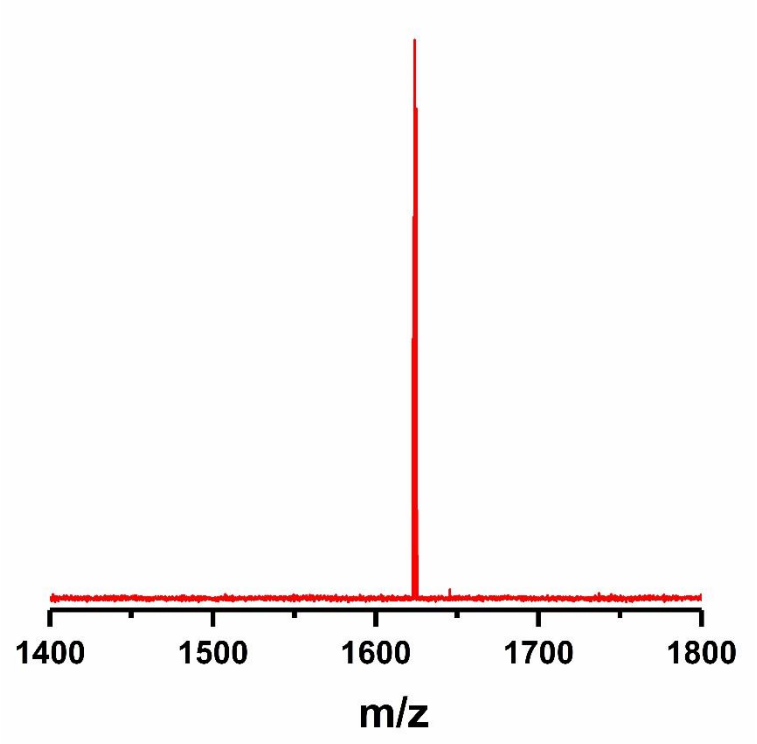

Figure S6. MALDI-TOF spectrum of the Boc-protected TTFPPP.

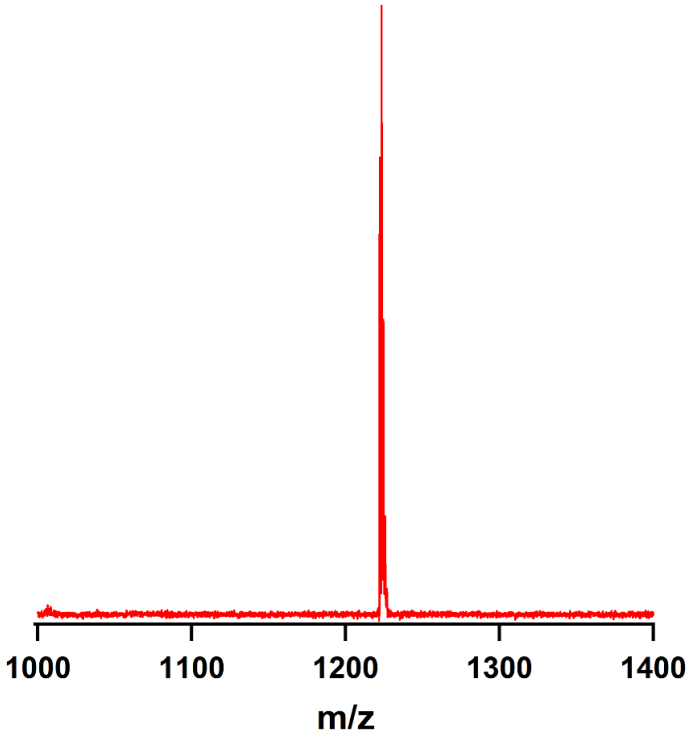

Figure S7. MALDI-TOF spectrum of TTFPPP **4**.

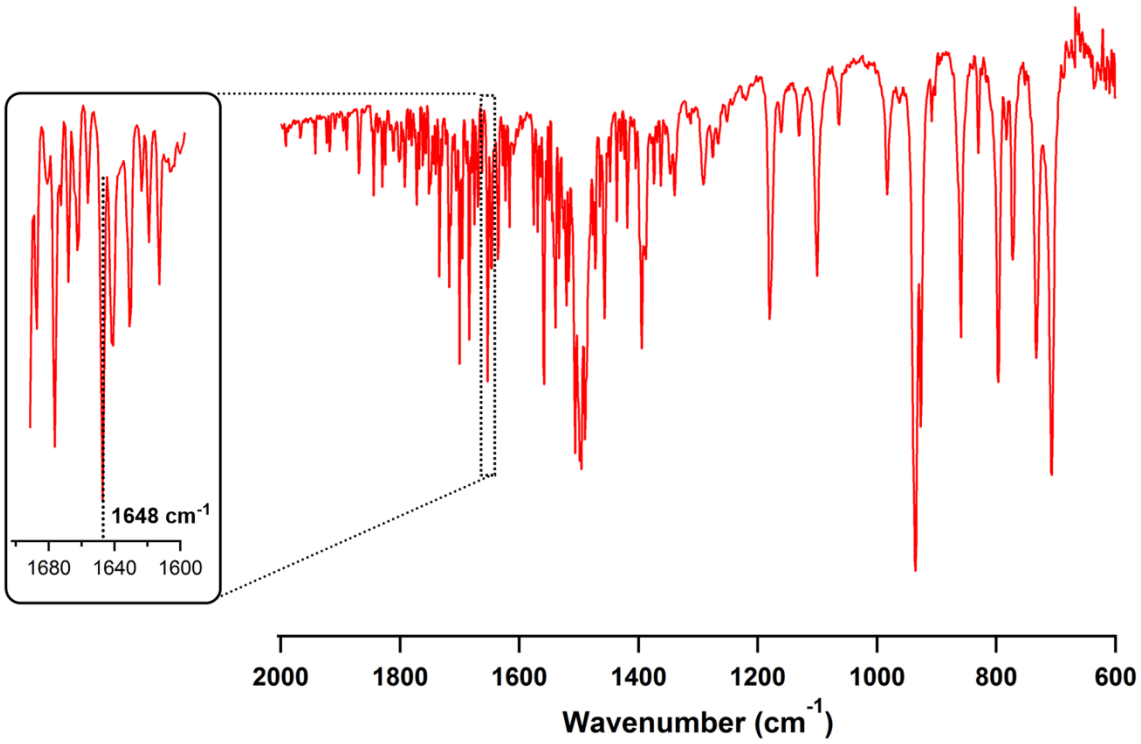

Figure S8. FT-IR spectrum of as-synthesized PCN-624 (peak at 1648 cm^{-1} was assigned to the C=N bond).

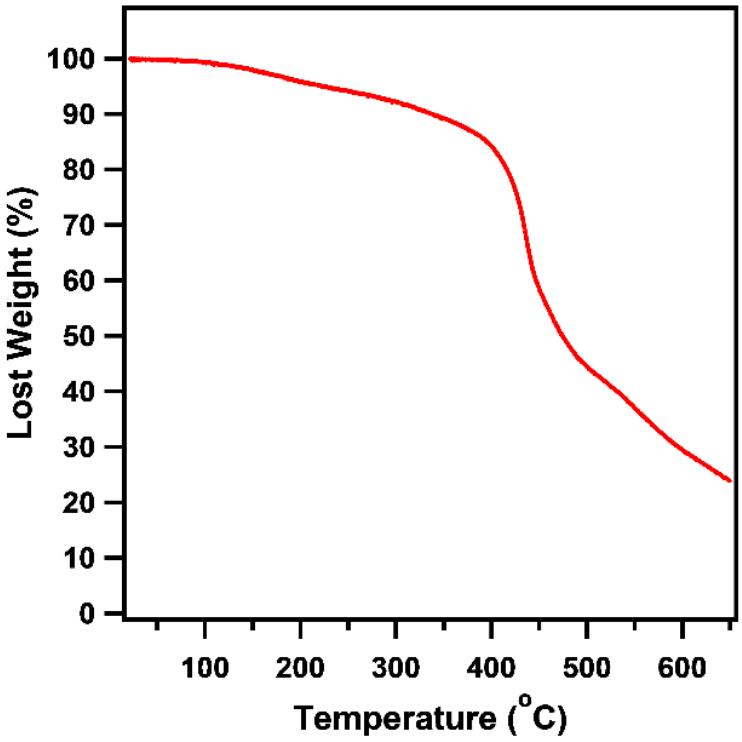

Figure S9. TGA analysis result of PCN-624 under N_2 atmosphere.

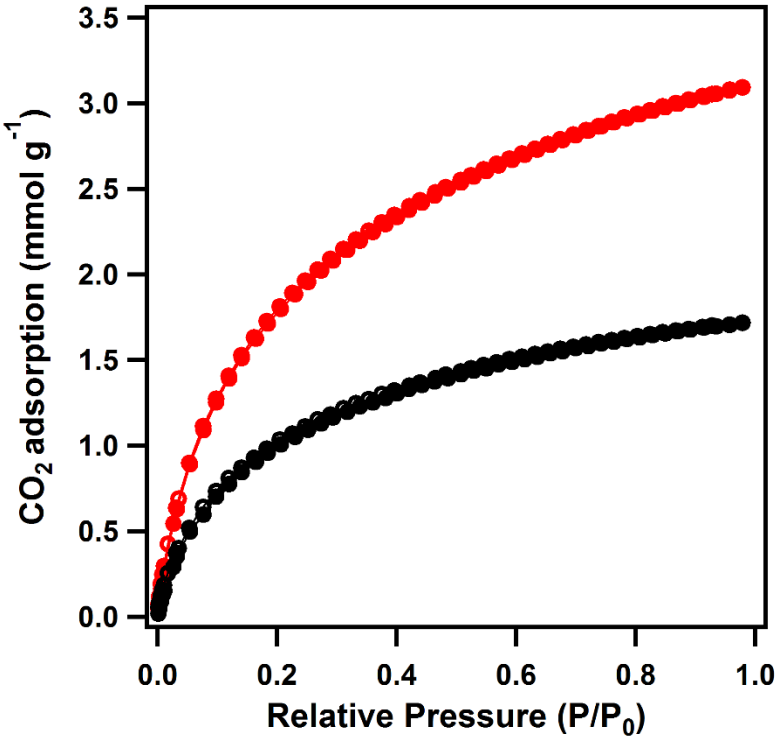

Figure S10. CO_2 sorption curves of PCN-624 at 298 K (black curve) and 273 K (red curve).

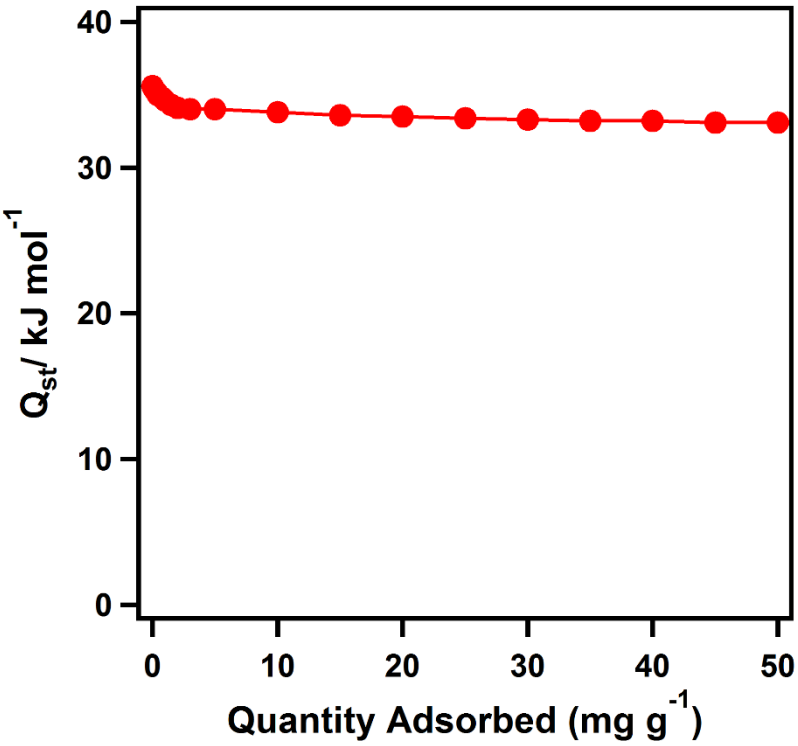

Figure S11. The heat of adsorption (Q_{st}) of PCN-624 for CO_2 sorption.

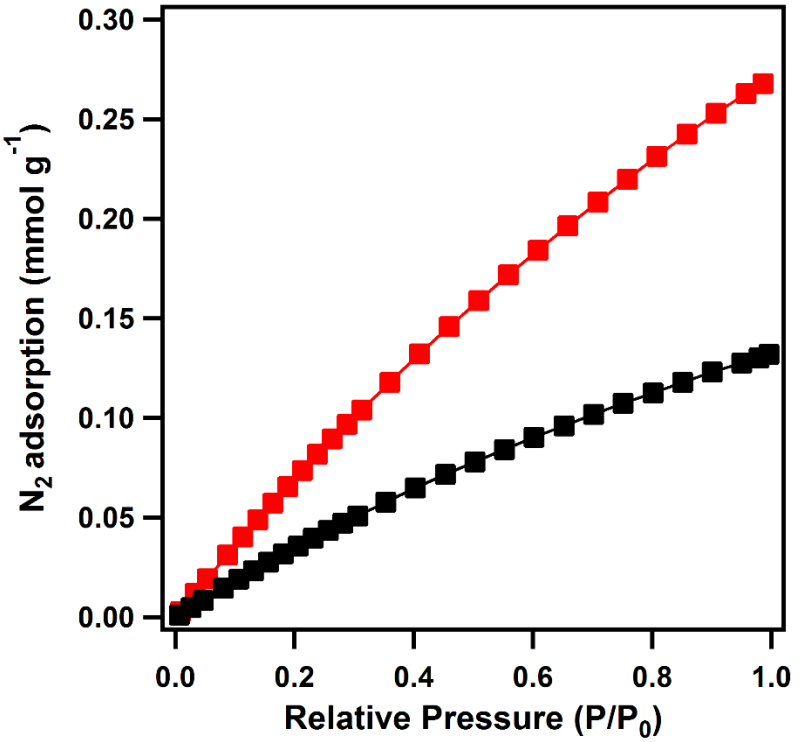

Figure S12. N_2 sorption curves of PCN-624 at 298 K (black curve) and 273 K (red curve).

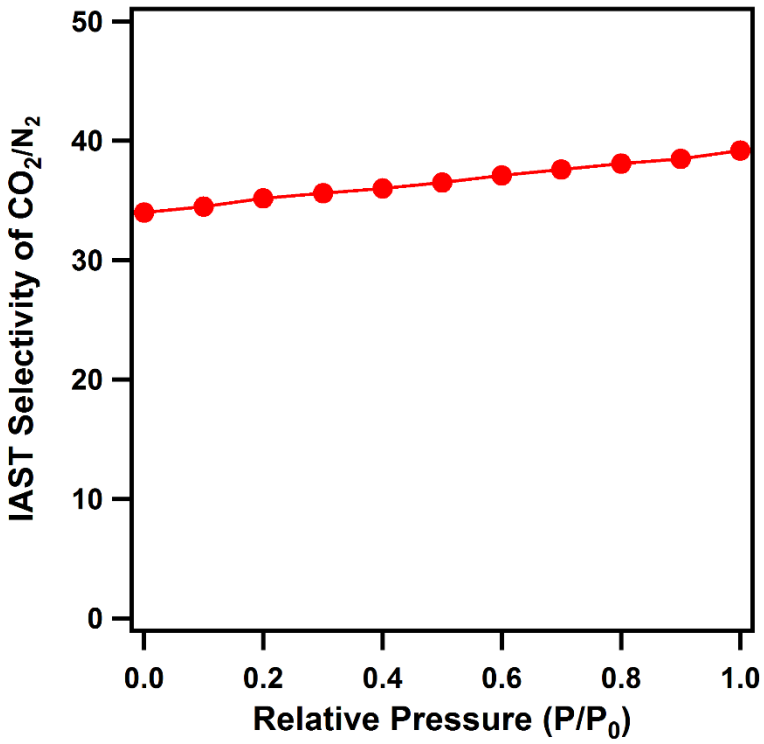

Figure S13. The IAST selectivity of PCN-624 for CO_2/N_2.

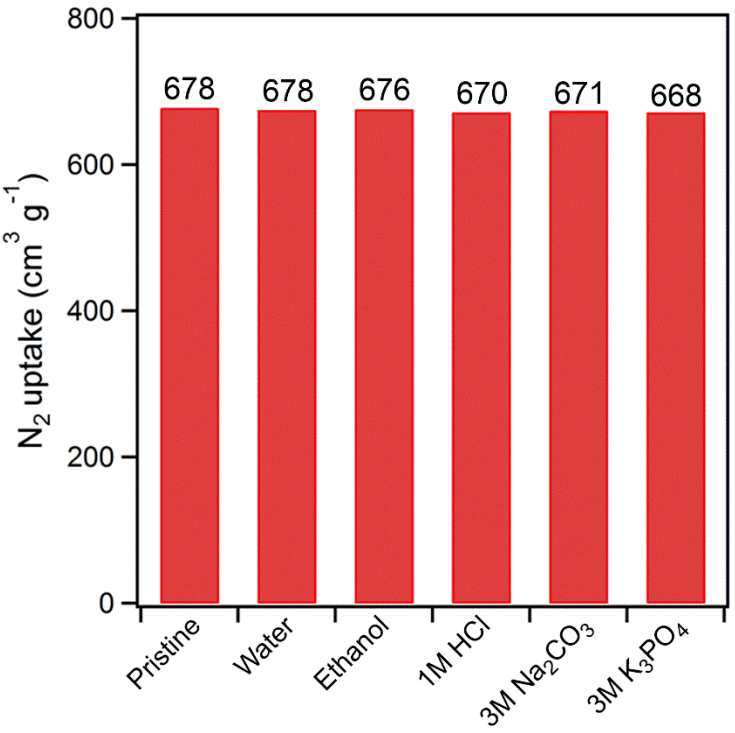

Figure S14. N_2 adsorption values of PCN-624 samples after treatment in different solutions.

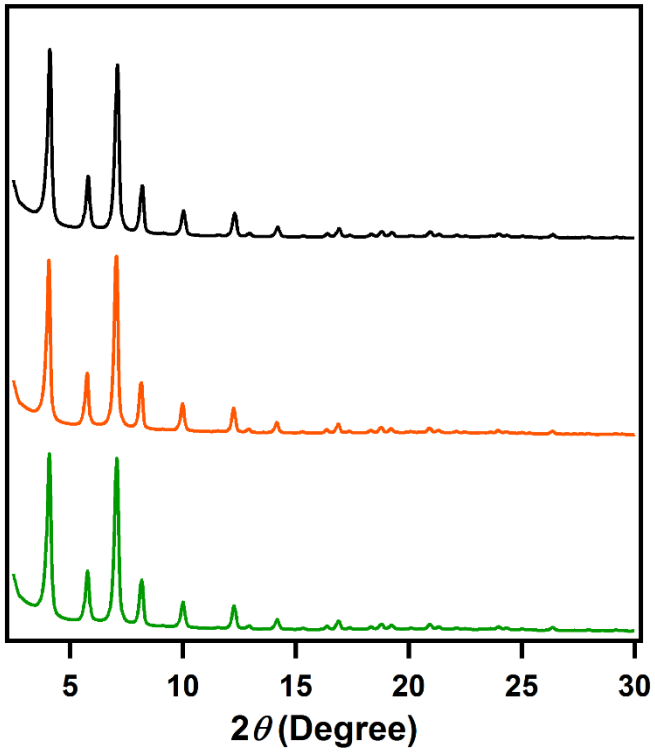

Figure S15. The PXRD patterns of PCN-624 after the treatment in HCl (1 M, black), Na_2CO_3 (3 M, orange), and K_3PO_4 (3 M, green) aqueous solution for four weeks.

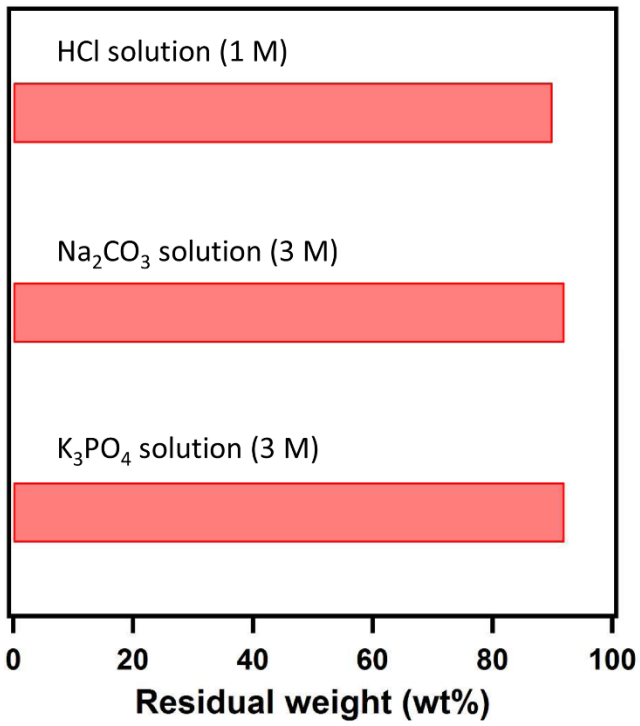

Figure S16. The residual weight of PCN-624 after the treatment in HCl (1 M), Na_2CO_3 (3 M), and K_3PO_4 (3 M) aqueous solution for four weeks.

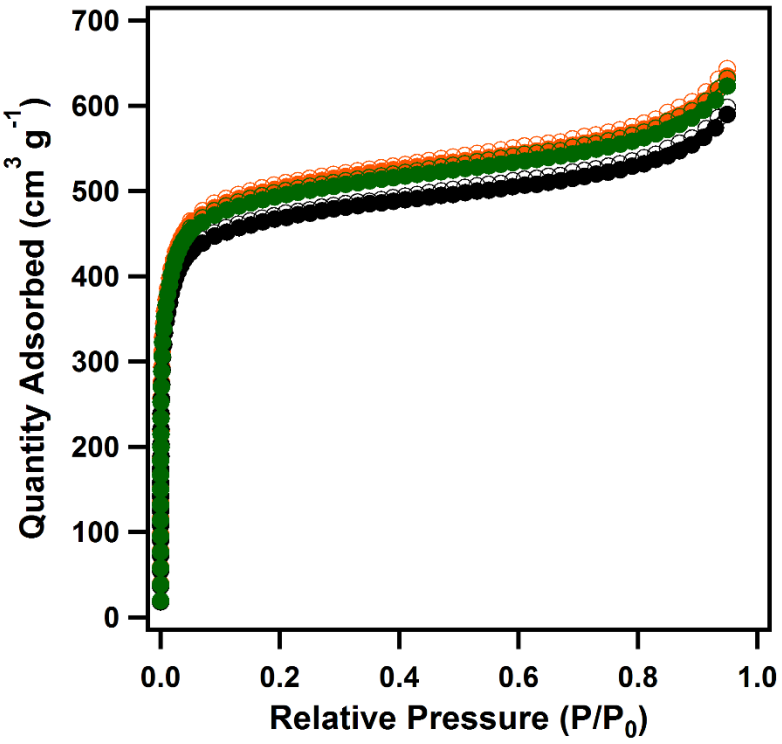

Figure S17. N_2 sorption curves of PCN-624 after the treatment in HCl (1 M, black), Na_2CO_3 (3 M, orange), and K_3PO_4 (3 M, green) aqueous solution for four weeks.

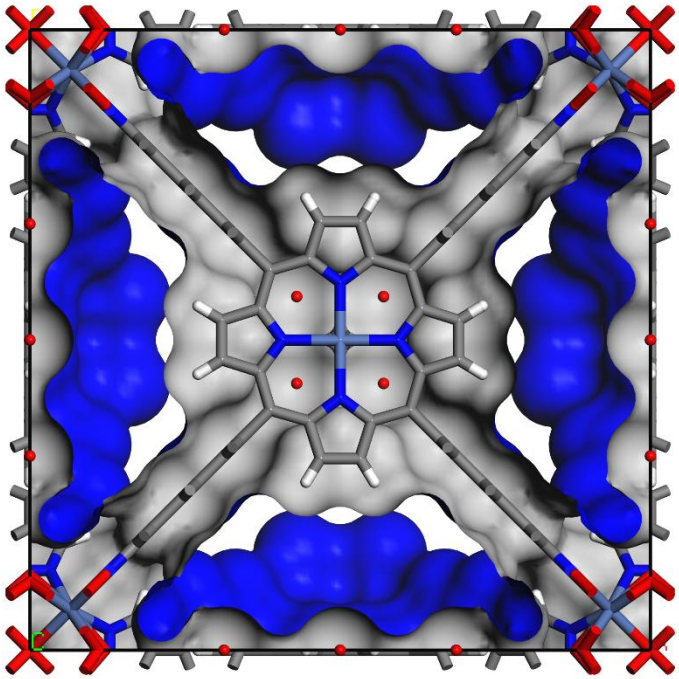

Figure S18. The void space within the crystal structure of PCN-624. Solvent accessible volumes of guest molecules were calculated with Material Studio 7.0, employing a probe radius of 2.4 Å.

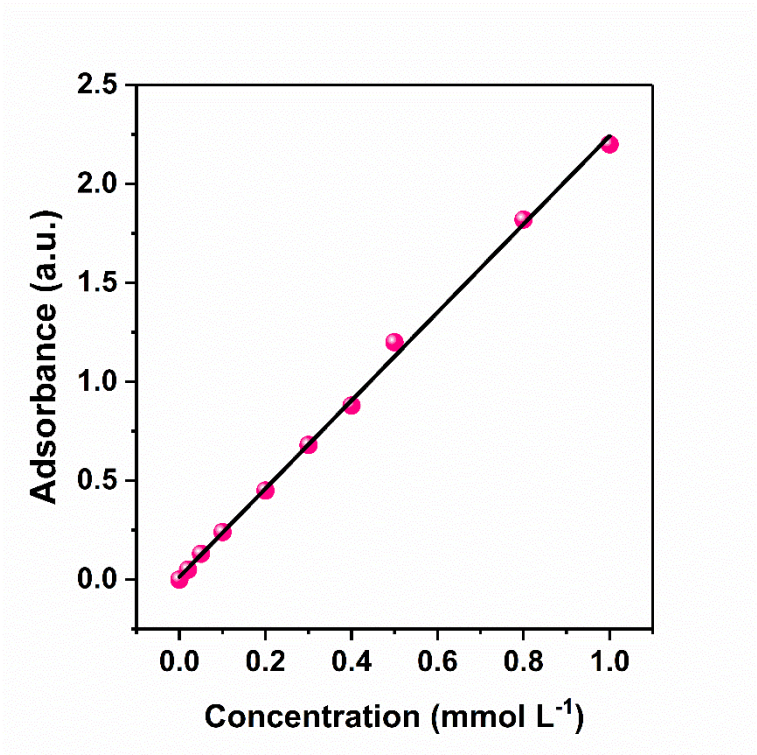

Figure S19. Beer-Lambert graph of $C_{60}An_2$ versus different concentrations in toluene.

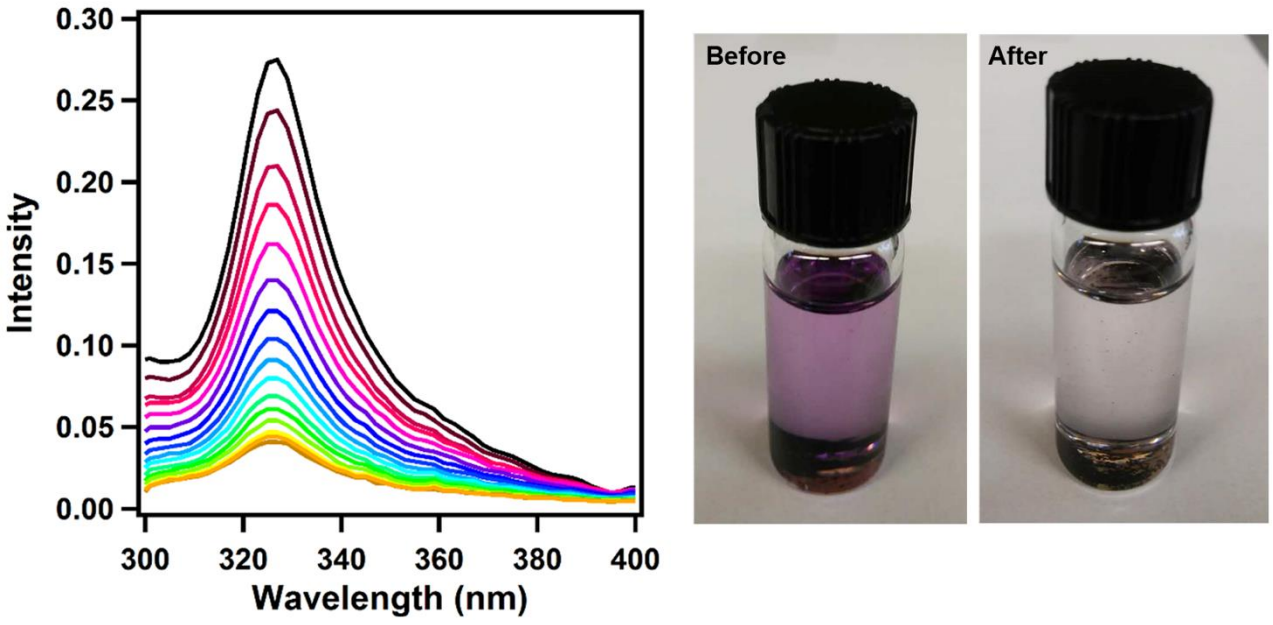

Figure S20. UV-Vis spectra of $C_{60}An_2$ after the adsorption of PCN-624 (left); the pictures of the $C_{60}An_2$ toluene solution before and after the adsorption of PCN-624 (right).

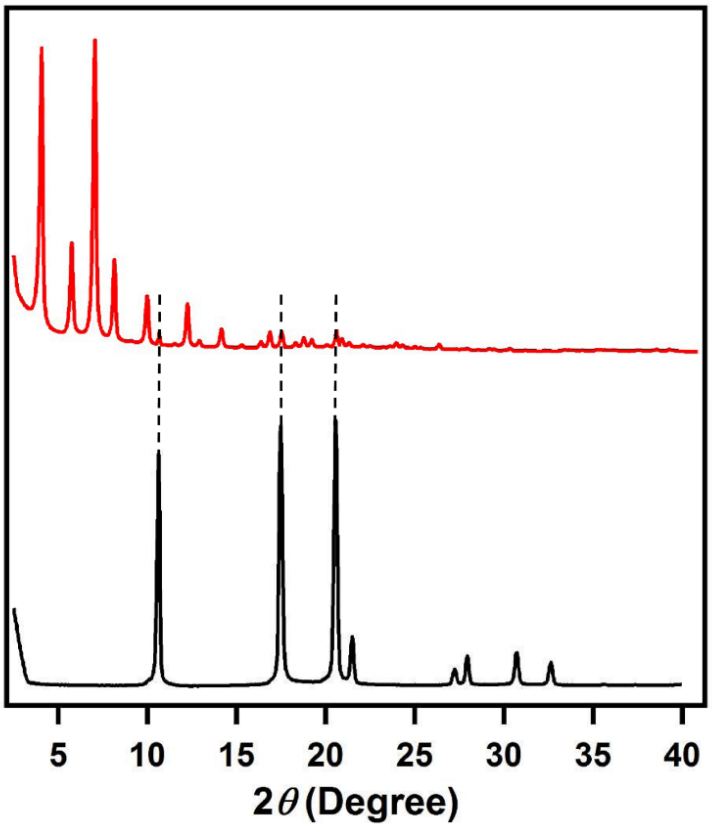

Figure S21. PXRD patterns of $C_{60}An_2$ (black curve) and $C_{60}An_2$⊂PCN-624 (red curve).

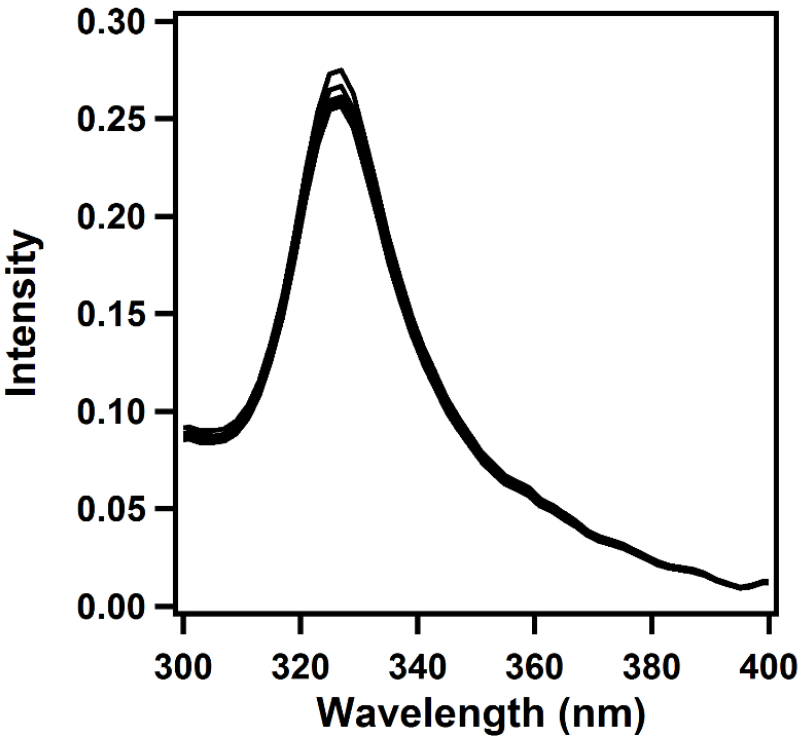

Figure S22. UV-Vis spectra of $C_{60}An_2$ after the adsorption of PCN-602.

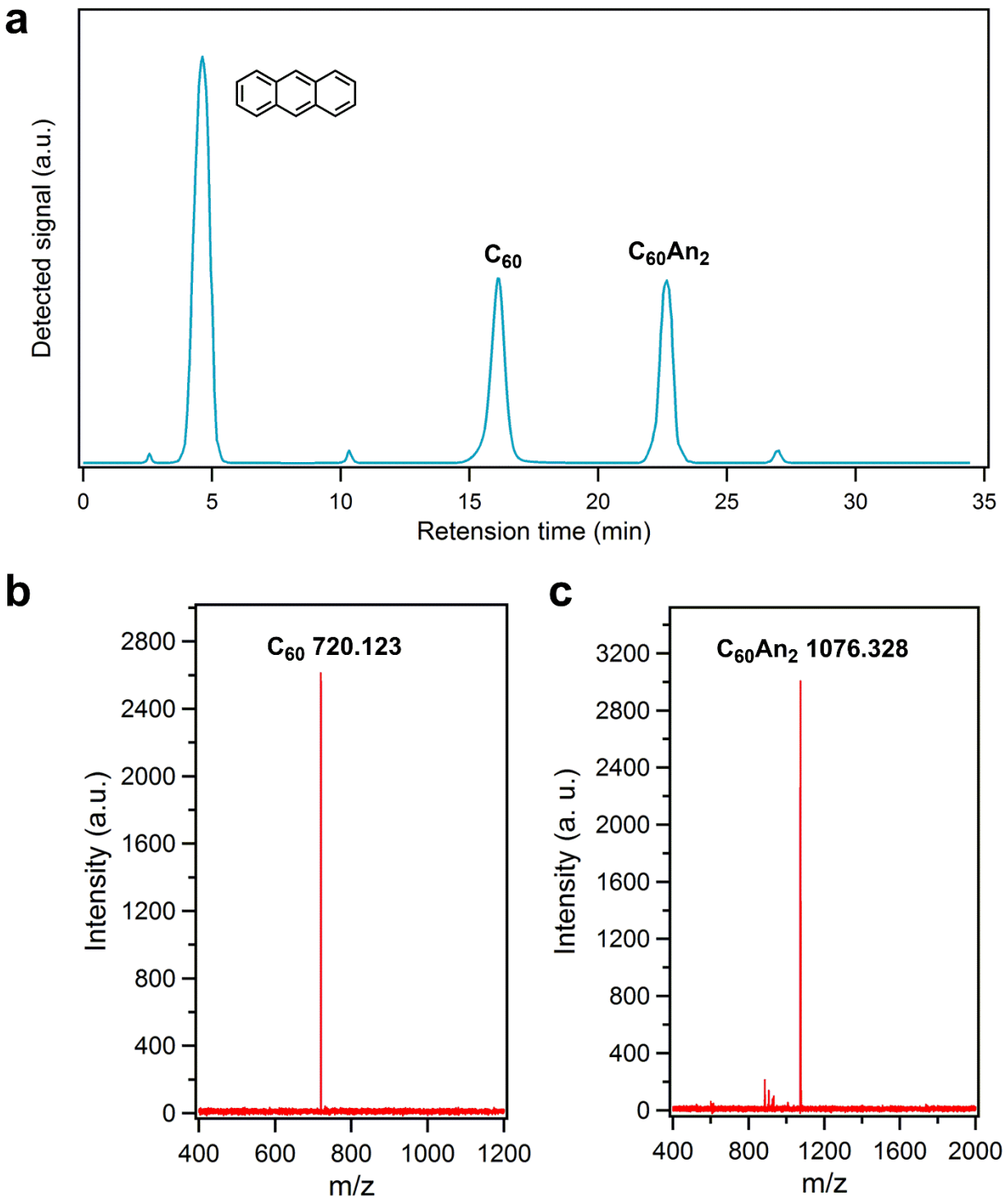

Figure S23. HPLC-MS spectra for the formation of $C_{60}An_2$ in presence of PCN-624. a) Analytical HPLC for the crude product, toluene 0.5 ml/min. b) MALDI-TOF MS for C_{60}. c) MALDI-TOF MS for $C_{60}An_2$.

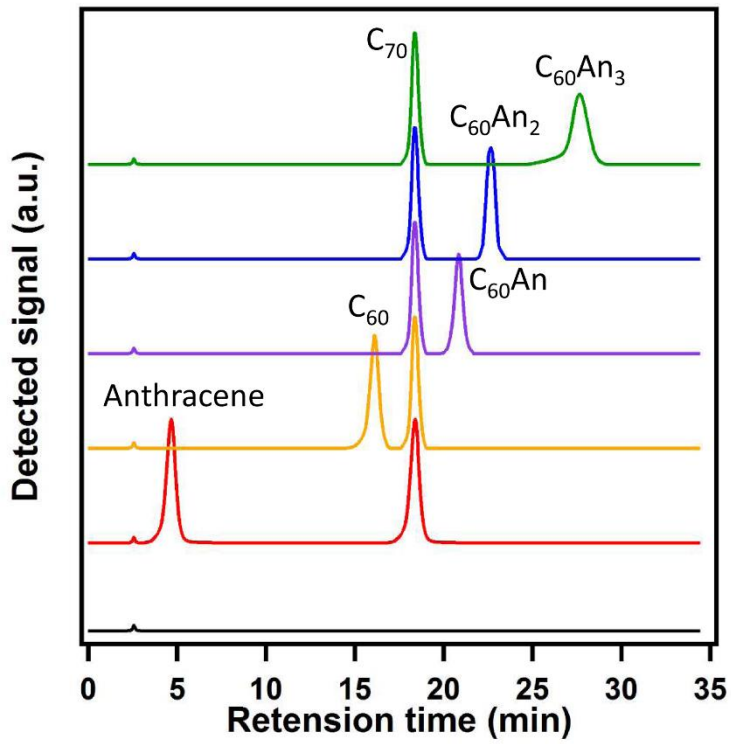

Compound	Time (min)	Peak width (min)	Symmetrical factors	Relative retention time (min)	Area	R.S.D. (%)
Anthracene	4.632	0.64	0.97	0.25	156324	3.43 (n=5)
C_{60}	16.097	0.66	1.00	0.87	132643	1.84 (n=5)
C_{70}	18.346	0.52	1.00	1.00	149553	1.97 (n=5)
$C_{60}An$	20.823	0.62	0.99	1.14	103266	2.42 (n=5)
$C_{60}An_2$	22.658	0.58	0.96	1.23	123264	3.12 (n=5)
$C_{60}An_3$	27.617	0.82	0.95	1.50	134166	2.37 (n=5)

Figure S24. The HPLC spectra of anthracene, C_{60}, $C_{60}An$, $C_{60}An_2$, and $C_{60}An_3$ with C_{70} as the internal standard.

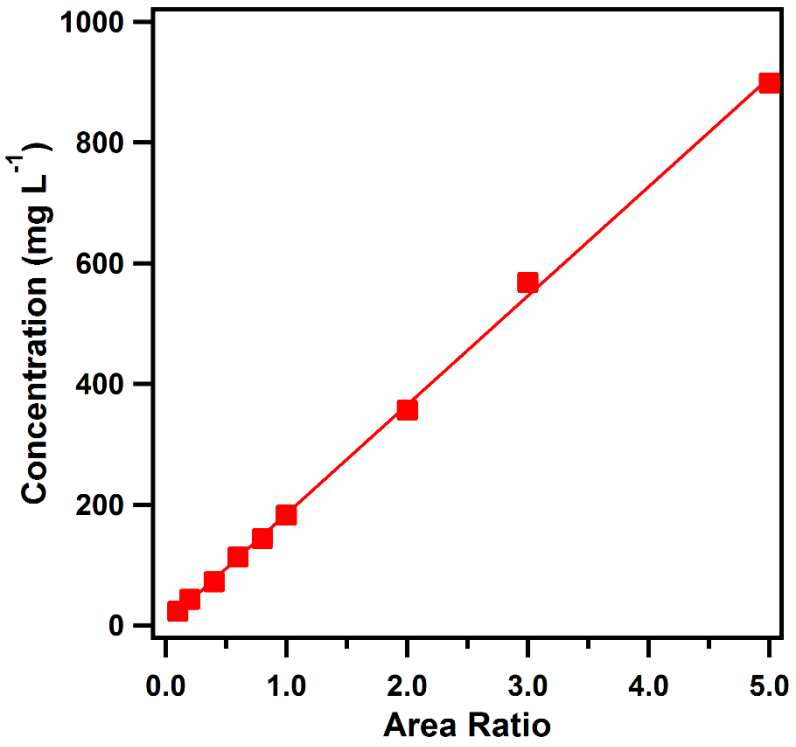

Figure S25. Standard curve of anthracene with C_{70} as the internal standard.

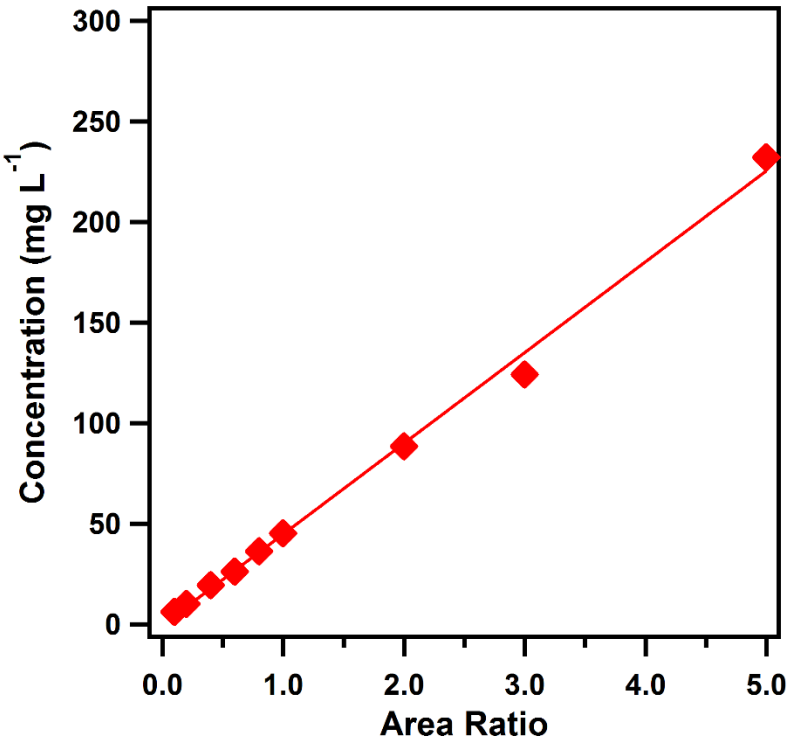

Figure S26. Standard curve of C_{60} with C_{70} as the internal standard.

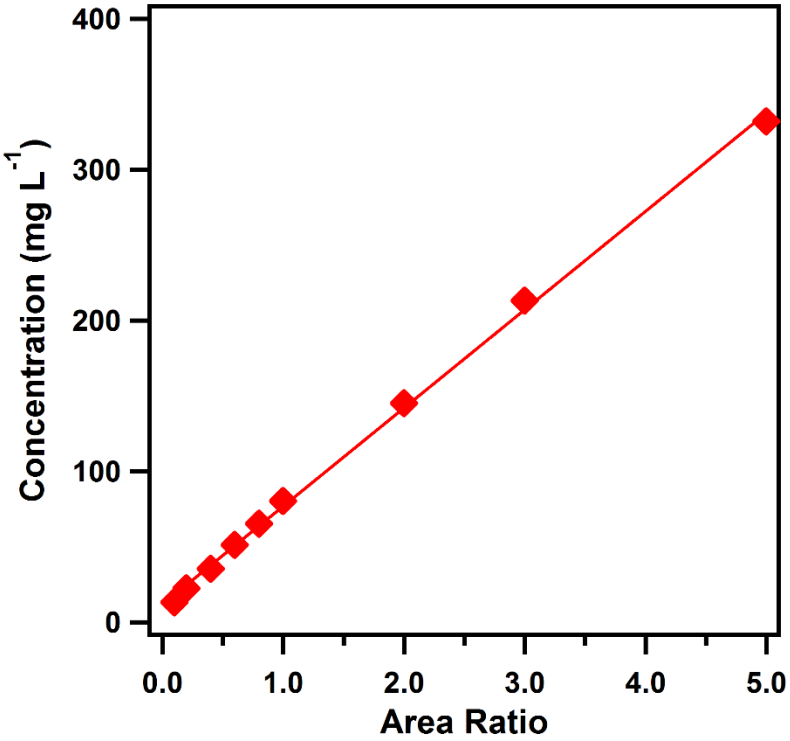

Figure S27. Standard curve of $C_{60}An$ with C_{70} as the internal standard.

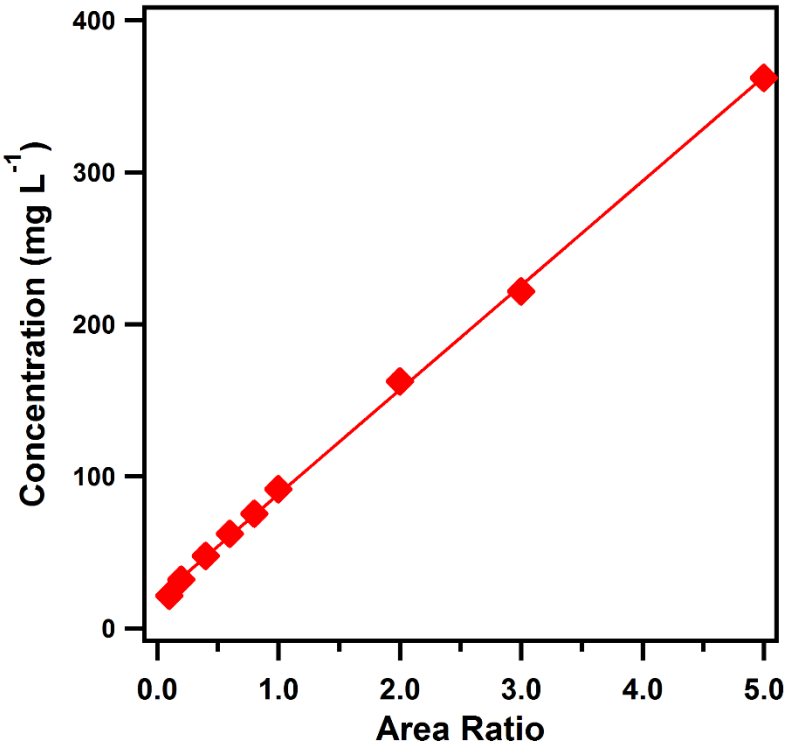

Figure S28. Standard curve of $C_{60}An_2$ with C_{70} as the internal standard.

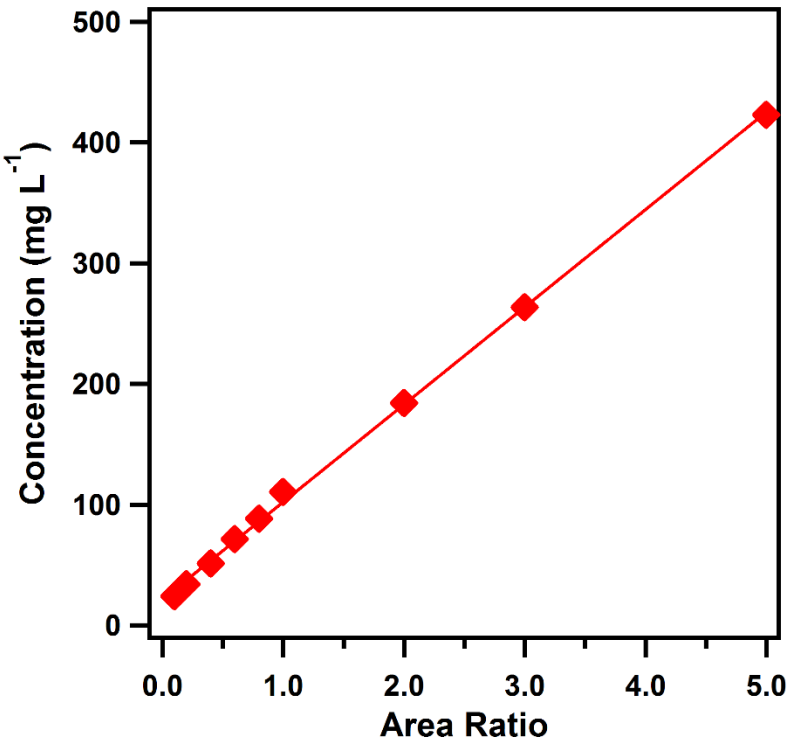

Figure S29. Standard curve of $C_{60}An_3$ with C_{70} as the internal standard.

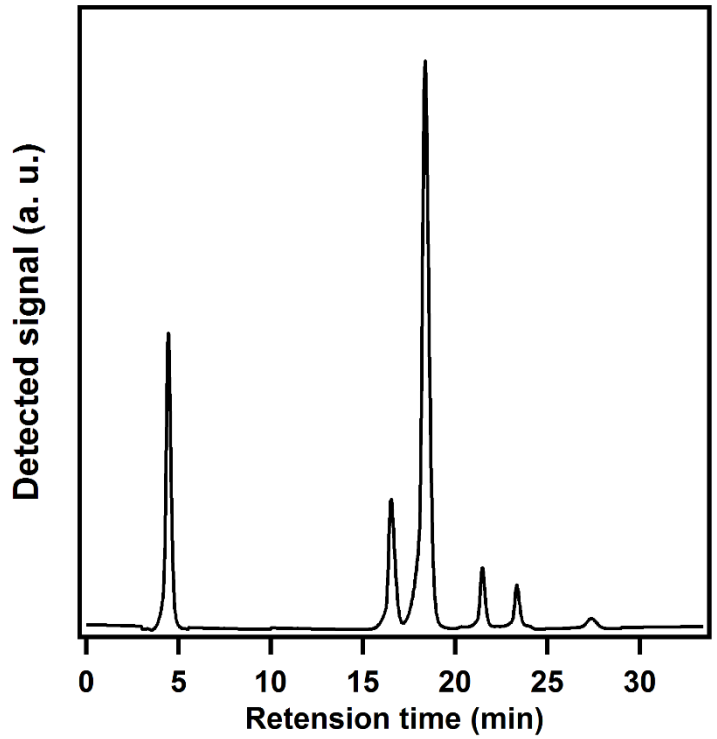

Figure S30. HPLC trace of the Diels–Alder reaction between anthracene and C_{60} catalyzed by PCN-624 (Table 1, entry 1).

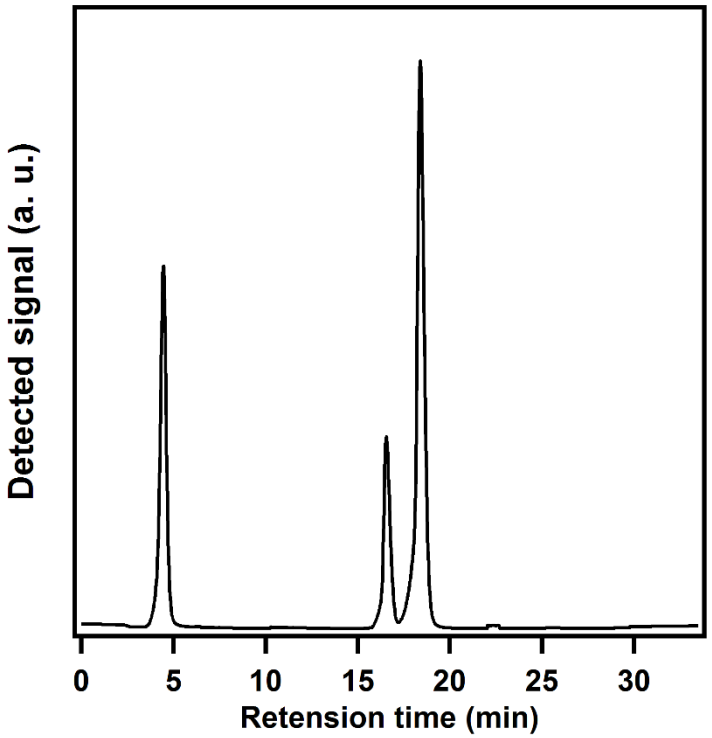

Figure S31. HPLC trace of the Diels–Alder reaction between anthracene and C_{60} catalyzed by PCN-624 (Table 1, entry 2).

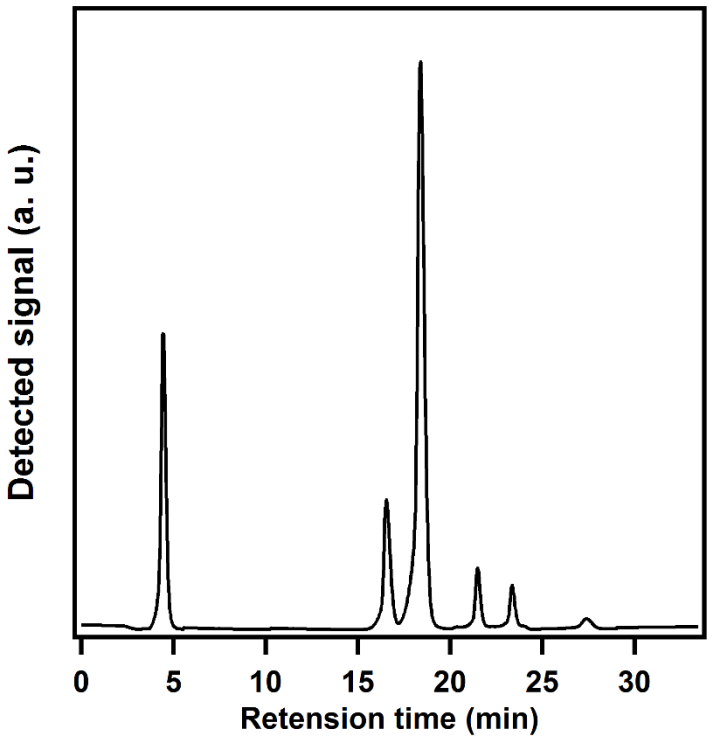

Figure S32. HPLC trace of the Diels–Alder reaction between anthracene and C_{60} catalyzed by PCN-624 (Table 1, entry 3).

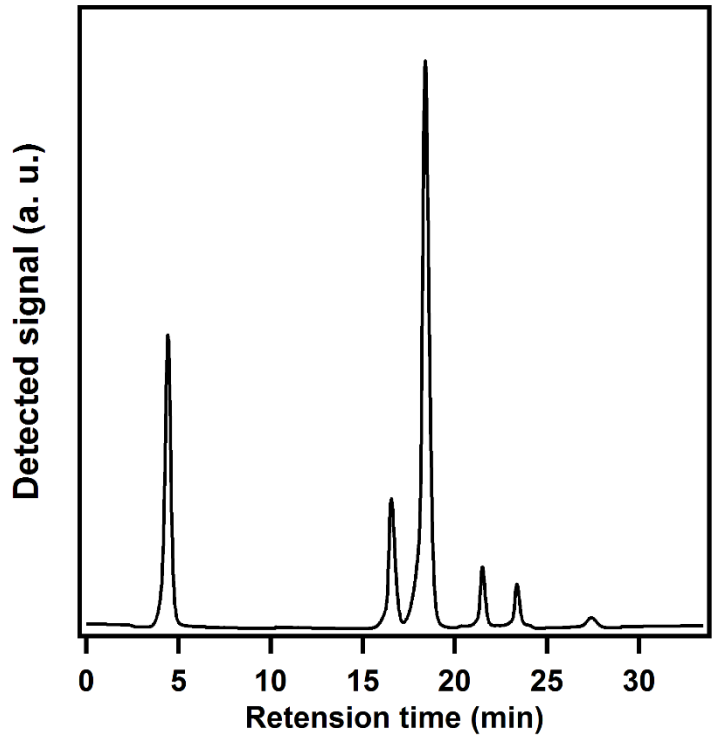

Figure S33. HPLC trace of the Diels–Alder reaction between anthracene and C_{60} catalyzed by PCN-624 (Table 1, entry 4).

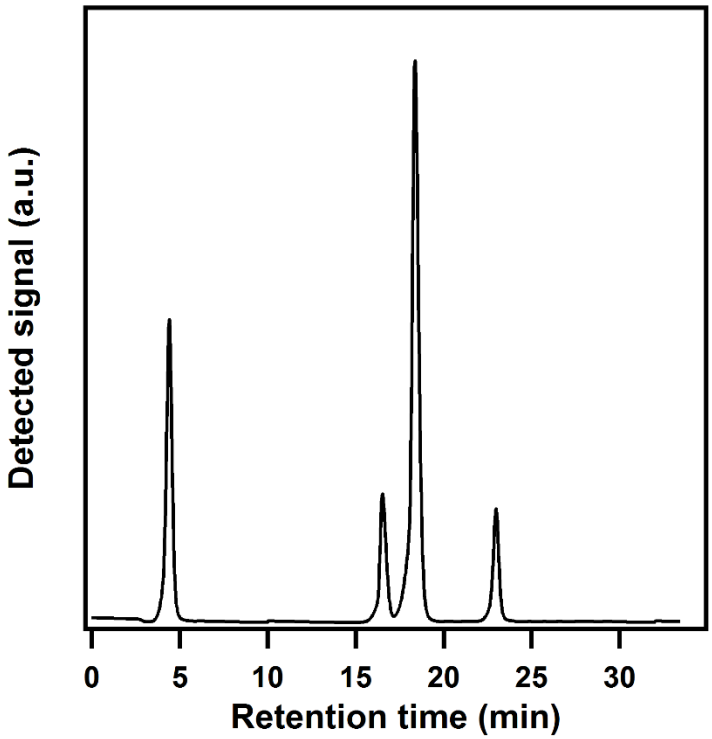

Figure S34. HPLC trace of the Diels–Alder reaction between anthracene and C_{60} catalyzed by PCN-624 (Table 1, entry 5).

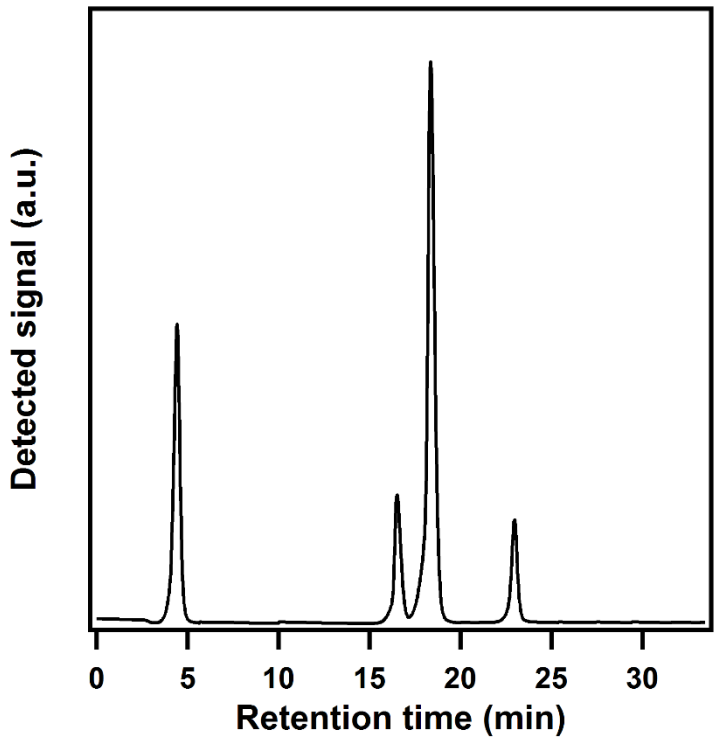

Figure S35. HPLC trace of the Diels–Alder reaction between anthracene and C_{60} catalyzed by PCN-624 (Table 1, entry 6).

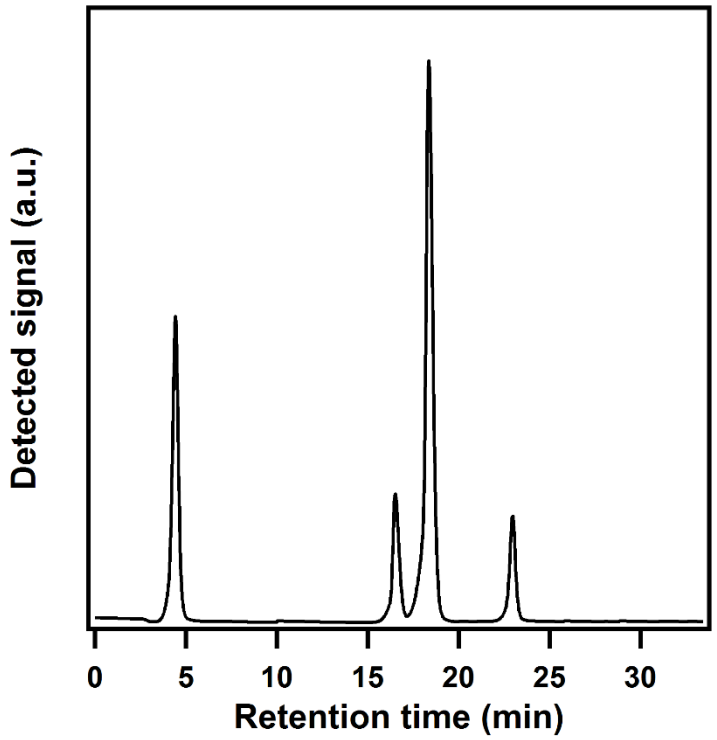

Figure S36. HPLC trace of the Diels–Alder reaction between anthracene and C_{60} catalyzed by PCN-624 (Table 1, entry 7).

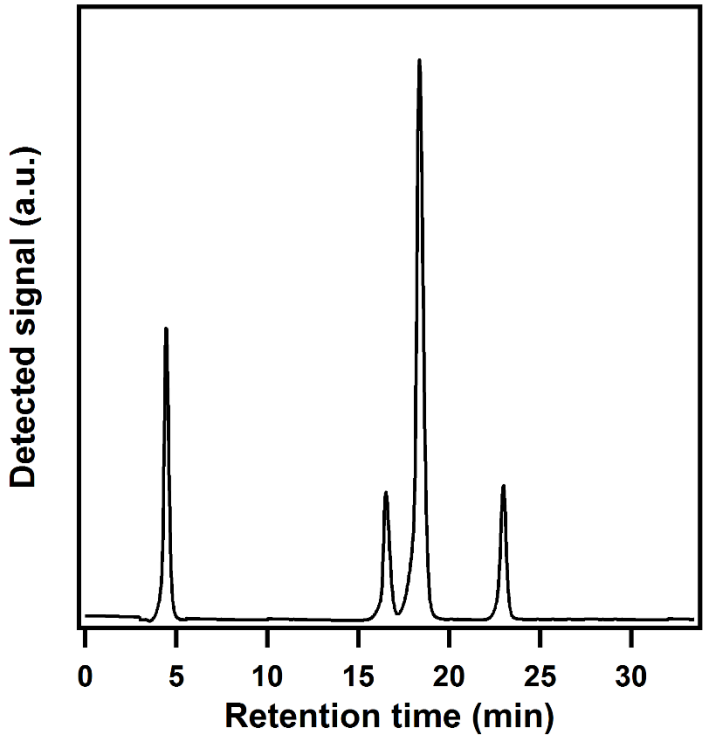

Figure S37. HPLC trace of the Diels–Alder reaction between anthracene and C_{60} catalyzed by PCN-624 (Table 1, entry 8).

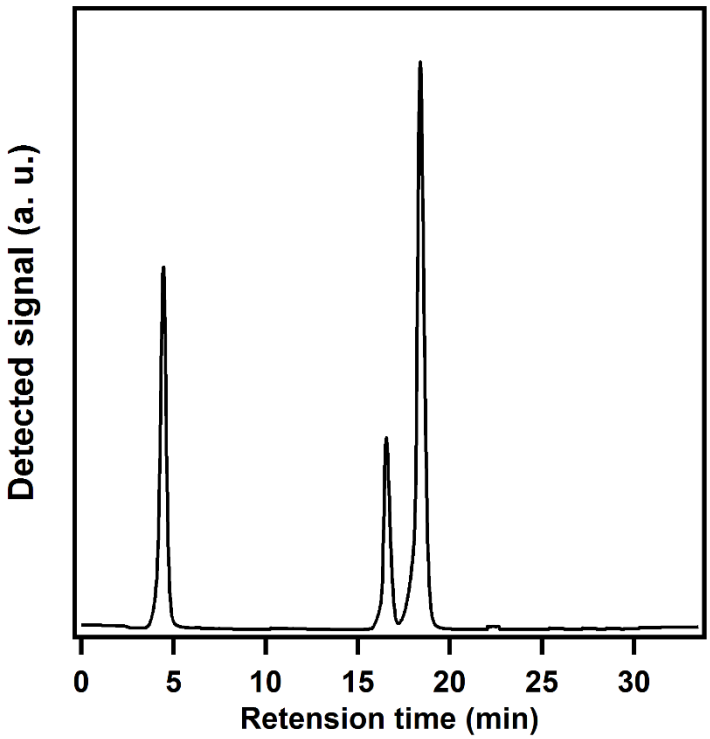

Figure S38. HPLC trace of the Diels–Alder reaction between anthracene and C_{60} catalyzed by PCN-624 (Table 1, entry 9).

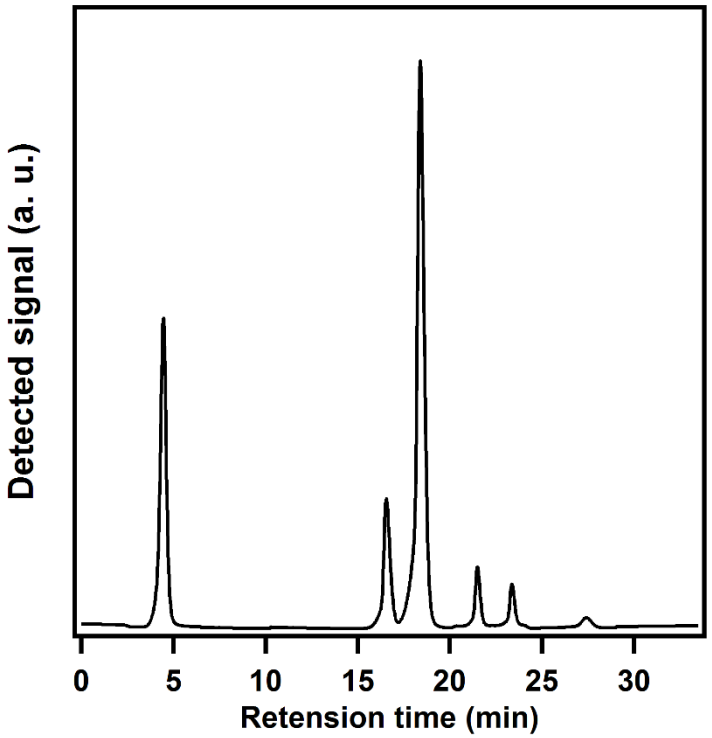

Figure S39. HPLC trace of the Diels–Alder reaction between anthracene and C_{60} catalyzed by PCN-624 (Table 1, entry 10).

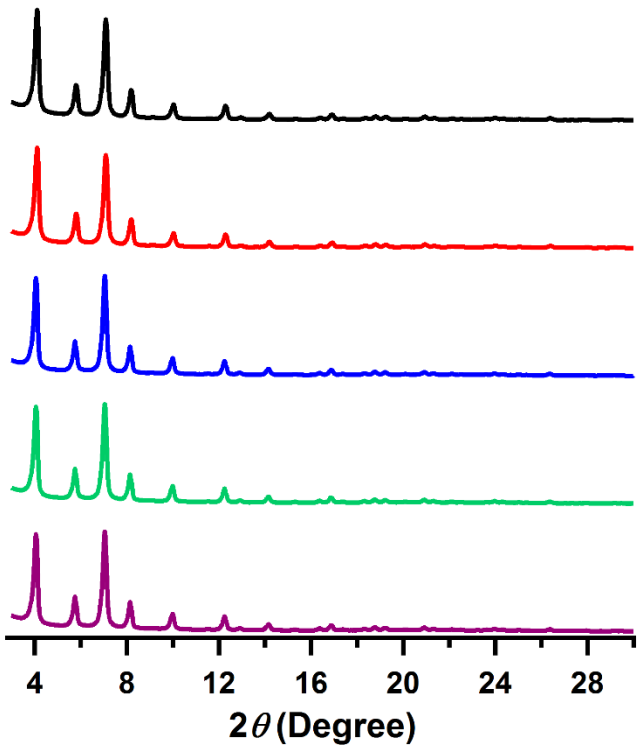

Figure S40. PXRD patterns of recycled PCN-624 samples (black curve, 1st run; red curve, 2nd run; blue curve, 3rd curve; green curve, 4th run; purple curve, 5th run).

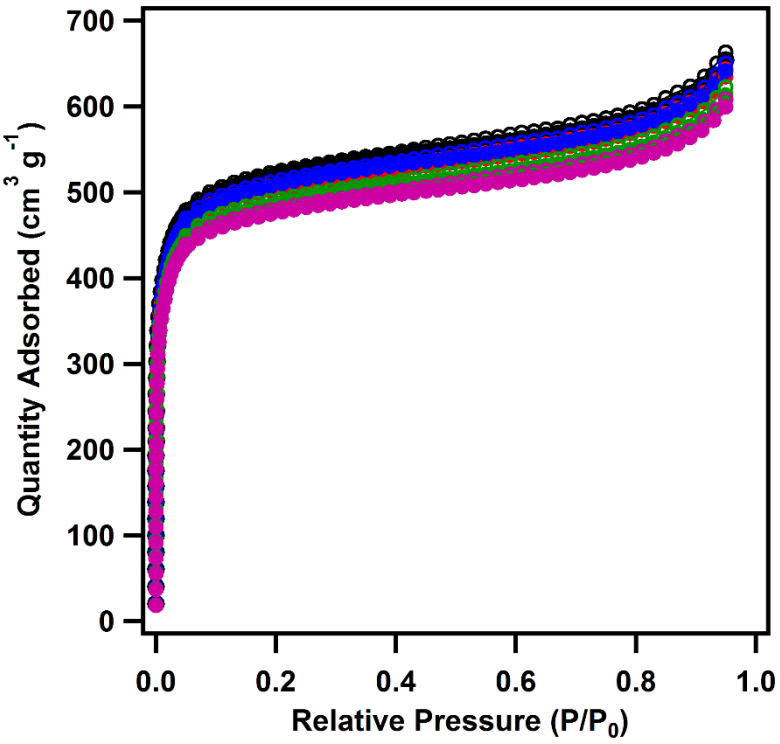

Figure S41. N_2 sorption isotherms of recycled PCN-624 samples (black curve, 1st run; red curve, 2nd run; blue curve, 3rd curve; green curve, 4th run; purple curve, 5th run).

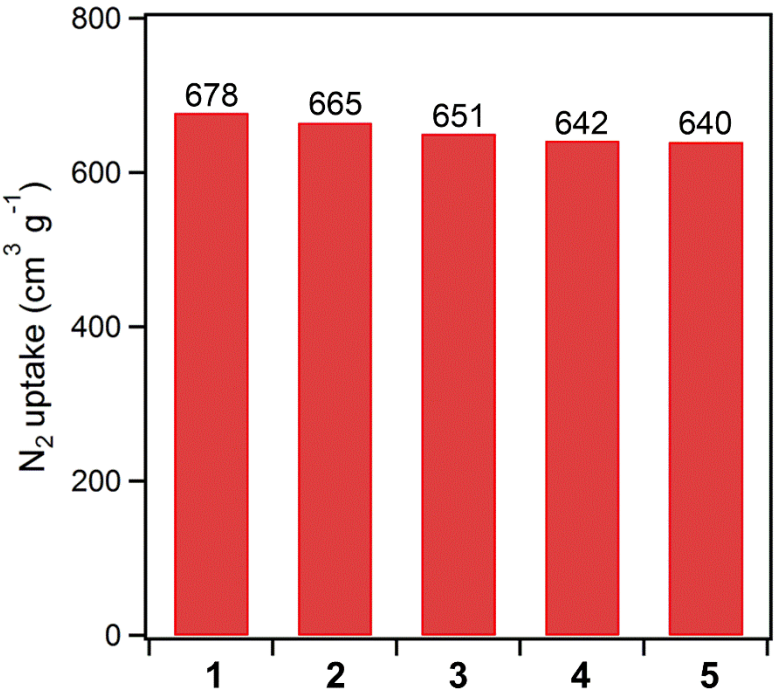

Figure S42. N_2 adsorption values of PCN-624 samples over the five cycles.

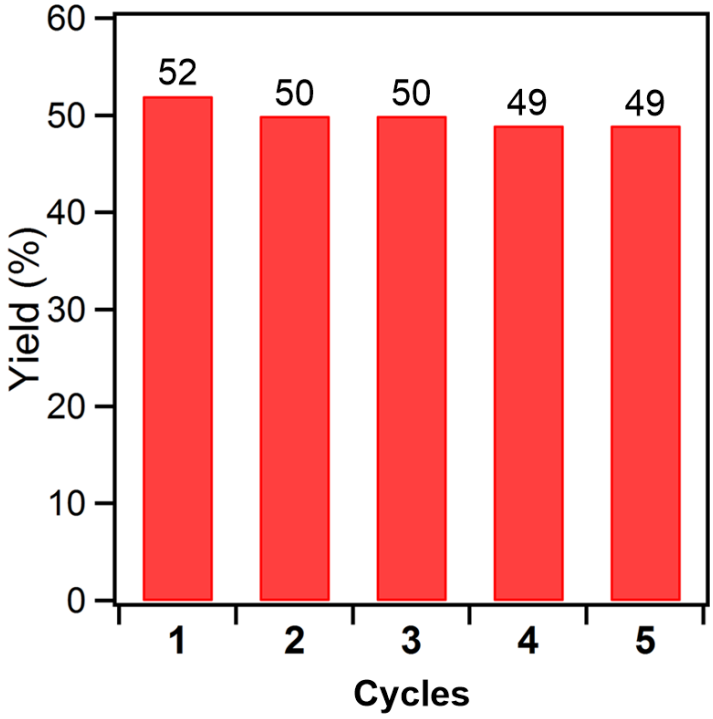

Figure S43. The recycling catalytic performance of PCN-624 in the selective synthesis of $C_{60}An_2$.

Section 4. Supporting Tables

Table S1. Unit cell parameters of PCN-624 determined via Pawley fitting of powder X-ray diffraction data.

MOF	PCN-624
Crystal system	cubic
Space group	Pm3−m
a, b, c / Å	21.836(4)
α, β, γ / °	90
V / $Å^3$	10411.64(2)
R_{exp}	0.432
R_{wp}	1.025
R_p	1.242
Wavelength (Å)	0.727680
Temperature	298 K

Table S2. Theoretical calculation results of solvent accessible volumes for guest molecules with a probe radius of 1.4 Å.[S4]

Guest Molecules	Solvent accessible volume	Cavity occupation of PCN-624 (%)
$C_{60}An_1$	681.3	21.4
$C_{60}An_2$-trans1	845.3	26.6
$C_{60}An_2$-trans2	854.4	26.8
$C_{60}An_2$-trans3	853.9	26.8
$C_{60}An_2$-trans4	852.4	26.8
$C_{60}An_2$-e'	850.4	26.7
$C_{60}An_2$-e"	856.9	26.9
$C_{60}An_3$	1021.5	32.1

Table S3. Elemental analysis of the products $C_{60}An$, $C_{60}An_2$, and $C_{60}An_3$.

Compound		C (%)	H (%)
$C_{60}An$	Calculated	98.88	1.12
	Found	98.74	1.16
$C_{60}An_2$	Calculated	98.13	1.87
	Found	98.08	1.90
$C_{60}An_3$	Calculated	97.59	2.41
	Found	97.51	2.45

Section 5. Supporting References

S1. Bischoff, A.; Sundaresan, K.; Koteswara, R. P. B.; Ainan, B.; Ayyamperumal, H.; A R, G.; Tatiparthy, S.; Prabhu, G.; Subramanya, H. *European Patent*. **2009**, EP2268143 A4.

S2. Tsuda, M., Ishida, T., Nogami, T., Kurono, S., Ohashi, M. *J. Chem. Soc., Chem. Commun*, **1993**, 1296−1298.

S3. Duarte-Ruiz, A., Müller, T., Wurst, K., Kräutler, B. *Tetrahedron* **2001**, *57*, 3709−3714.

S4. Brenner, W.; Ronson, T. K.; Nitschke, J. R. *J. Am. Chem. Soc.* **2017**, *139*, 75−78.